



Note

Effect of the axial halogen ligand on the substitution reactions of chromium(III) porphyrin complex

Kikuko Okada, Atsumi Sumida, Rie Inagaki, Masahiko Inamo*

Department of Chemistry, Aichi University of Education, Hiroosawa 1, Igaya, Kariya 448-8542, Japan

ARTICLE INFO

Article history:

Received 7 May 2011

Received in revised form 29 March 2012

Accepted 1 April 2012

Available online 6 April 2012

Keywords:

Metalloporphyrin

Chromium(III)

Substitution reaction

Trans effect

ABSTRACT

The thermodynamics and kinetics of the substitution reaction of the chromium(III) complex of 5,10,15,20-tetraphenylporphyrin, [Cr(TPP)(X)(L)] (X = F, Cl, Br), where L represents a non-charged ligand such as H₂O, pyridine, or 1-methylimidazole, was investigated. The present study aimed to elucidate the effect of the axial halogen ligand, X on the substitution reaction of the ligand trans to X. The substitution reaction of the axial pyridine ligand of [Cr(TPP)(X)(Py)] by 1-methylimidazole was studied spectrophotometrically in dichloromethane, and it was found that the reaction proceeds via a limiting dissociative mechanism and the activation enthalpy of the dissociation of pyridine is much smaller for the fluorine complex, [Cr(TPP)(F)(Py)], than for the chlorine complex, [Cr(TPP)(Cl)(Py)], i.e., $\Delta H^\ddagger = 57.5 \pm 1.1$ and 97.2 ± 1.4 kJ mol⁻¹, respectively. These results are discussed in terms of the trans effect of the halogen ligand on the axial ligand substitution reaction of [Cr(TPP)(X)(L)], and it is concluded that the strength of the bond shows the tendency of Cr–F > Cr–Cl > Cr–Br, leading to the strong trans effect of the F⁻ ligand.

© 2012 Elsevier B.V. All rights reserved.

1. Introduction

The chemistry of metalloporphyrins has been extensively studied for many years in relation to the naturally occurring tetrapyrrole macrocyclic compounds in various biological systems. One of the characteristic features of metalloporphyrins caused by porphyrin ligation is acceleration of the axial ligand substitution reaction, which is closely related to biological functions such as oxygen transport and storage by heme proteins, and this labilization effect reaches more than several orders of magnitude, especially in reactions with the usually substitution – inert chromium(III) [1–13], cobalt(III) [14–26], and rhodium(III) [27,28] ions. In order to elucidate the mechanism of the labilization effect of the porphyrin ligand, axial substitution reactions of metalloporphyrins have been extensively studied. O'Brien et al. studied the axial ligand substitution reactions of chromium(III) porphyrin complexes in a non-coordinating organic solvent [6] and was revealed that the axial substitution reaction proceeds via a limiting dissociative mechanism that includes a coordinately unsaturated complex as a reactive intermediate based on the kinetics of the reaction. It is desirable to study the chemical properties of a reactive intermediate directly in elucidating the intrinsic reaction mechanism, and photochemical studies using the laser photolysis technique have been successfully applied to these reaction systems, confirming the extremely high reactivity of the coordinately unsaturated intermediate [29–36].

Besides these photochemical studies, we also reported the substituent effect of the axial ligand on the substitution reaction of the Cr(III) porphyrin complex. The effect of β and γ substituents of the pyridine ligand on the dynamics of the substitution reaction was discussed in terms of the electronic effect caused by the substituents [12]. On the other hand, the presence of a steric strain of the methyl group bound at the α position of the coordinating nitrogen atom of imidazole was found to result in acceleration of the dissociation reaction of the ligand, as well as a decrease in the binding constant of the imidazole ligand to the metalloporphyrin [13]. These findings are in accord with the increase in the bond length between the chromium and nitrogen atoms induced by the steric strain due to the α -methyl substituent of the imidazole ligand. As an extension of our study, we investigated the kinetics of the axial ligand substitution reaction of [Cr(TPP)(X)(L)] (X = F, Cl, Br; L = H₂O, pyridine, 1-methylimidazole) in the dichloromethane solution spectrophotometrically. The purpose of the present study is to investigate the dynamics of the substitution reaction of the non-charged axial ligand trans to the halogen atom of the Cr(III) porphyrin complex in order to gain insight into the effect of the trans halogen ligand on the dynamics of the axial substitution reaction.

2. Experimental

2.1. Reagents

Pyridine (Py) and 1-methylimidazole (1-Melm) dried over solid potassium hydroxide were distilled before use. Spectroscopic

* Corresponding author. Tel./fax: +81 566 26 2636.

E-mail address: minamo@aeu.ac.jp (M. Inamo).

grade dichloromethane (Nacalai Tesque, Inc.) was used without further purification.

2.2. Preparation of [Cr(TPP)(F)(H₂O)]

Aquafluoro(5,10,15,20-tetraphenyl-porphyrinato)chromium (III), [Cr(TPP)(F)(H₂O)] was prepared according to a procedure similar to that of [Cr(TPP)(Cl)(H₂O)] [29,37]. Crude [Cr(TPP)(Cl)(H₂O)] (200 mg) was dissolved in chloroform and filtered. The filtrate was then applied to a column of activated alumina (Merck, neutral, 70–230 mesh) and eluted with chloroform. A slowly moving green band was collected, and the volume of the solution was reduced to about 50 cm³ on a rotary evaporator. Diluted hydrofluoric acid (20%, 5 cm³) was added to the chloroform solution, and the mixture was vigorously stirred for 30 min. The organic layer was separated and washed with water three times. Chloroform was removed on a rotary evaporator. The obtained solid was purified by column chromatography using silica gel (Merck, 0.040–0.063 mm) and eluted with chloroform containing 2% methanol. The green band was collected, and the solvent was evaporated to dryness. The solid was recrystallized from chloroform/hexane and dried under vacuum at room temperature for several hours. Fifty-five milligrams of a dark violet microcrystalline solid was obtained. *Anal. Calc.* for C₄₆H₃₂N₄O₂CrF ([Cr(TPP)(F)(H₂O)]·H₂O): C, 73.43; H, 4.48; N, 7.78. *Found:* C, 73.42; H, 4.43; N, 7.79%.

2.3. Preparation of [Cr(TPP)(Br)(H₂O)]

Aquabromo(5,10,15,20-tetraphenyl-porphyrinato)chromium (III), [Cr(TPP)(Br)(H₂O)] was prepared according to a method similar to that for [Cr(TPP)(F)(H₂O)] using hydrobromic acid instead of hydrofluoric acid. A mixture of toluene and hexane was used as the solvent for recrystallization. *Anal. Calc.* for C₄₄H₃₀N₄OBr ([Cr(TPP)(Br)(H₂O)]): C, 69.30; H, 3.96; N, 7.35. *Found:* C, 69.08; H, 4.40; N, 6.98%.

2.4. Preparation of [Cr(TPP)(Py)₂](ClO₄)

The pyridine adduct of the Cr(III)–TPP complex, [Cr(TPP)(Py)₂](ClO₄), was synthesized by reaction of the perchlorate salt of the Cr(III)–TPP complex. The chloride ion in [Cr(TPP)(Cl)(H₂O)] was substituted by the perchlorate ion by the following method. Crude [Cr(TPP)(Cl)(H₂O)] (100 mg) was dissolved in 10 cm³ of chloroform and filtered. The filtrate was then applied to a column of activated alumina (Merck, neutral, 70–230 mesh) and eluted with chloroform. A green band was collected, and the volume of the solution was reduced to about 50 cm³ on a rotary evaporator. Perchloric acid (20%, 6 cm³) was added to the chloroform solution, and the mixture was vigorously stirred for 20 min. The organic layer was separated, and chloroform was removed on a rotary evaporator. The solid was recrystallized from the mixed solvent of methanol and water and dried under vacuum at room temperature for several hours. Thirty-five milligrams of a dark violet microcrystalline solid was obtained. *Anal. Calc.* for C₄₆H₃₈N₄O₇CrCl ([Cr(TPP)](ClO₄)·2CH₃OH·H₂O): C, 65.29; H, 4.53; N, 6.62. *Found:* C, 65.09; H, 4.79; N, 6.49%. Two methanol molecules or methanol and water molecules may coordinate to the central chromium atom at the axial coordination sites. The perchlorate compound thus obtained (30 mg) and pyridine (60 mg) was dissolved in 6 cm³ of chloroform, and toluene (12 cm³) was then added to the solution. Dark violet crystals of [Cr(TPP)(Py)₂](ClO₄) were obtained by slow evaporation of the chloroform–toluene solution. *Anal. Calc.* for [Cr(TPP)(Py)₂](ClO₄): C, 70.32; H, 4.15; N, 9.11. *Found:* C, 70.04; H, 4.13; N, 8.93%.

2.5. Kinetic measurements

UV–Vis absorption spectra were recorded on a Hitachi U-3000 spectrophotometer. Kinetics of the axial substitution reaction of the porphyrin complex was studied by following the change of the UV–Vis absorption spectrum with time. The concentrations of the leaving and entering ligands were kept in large excess over that of the chromium(III) porphyrin complex to guarantee the pseudo-first-order conditions. The total concentration of the complex was in the range of (0.3–1.0) × 10^{−5} mol kg^{−1}. The absorbance, *A*, was followed after mixing the solution of the porphyrin complex and that of the entering ligand to determine the pseudo-first-order rate constant, *k*_{obsd}, according to Eq. (1)

$$A = A_{\infty} - (A_{\infty} - A_0) \exp(-k_{\text{obsd}}t) \quad (1)$$

where *A*_∞ and *A*₀ are the absorbances at *t* = ∞ and 0, respectively. The reproducibility of the *k*_{obsd} values was better than ±5%. The temperature of the reaction solutions was controlled to within ±0.1 °C using a circulating water bath with a thermostat. The concentration of water in the dichloromethane solution, which was determined by a Karl-Fischer titrator (CA-06, Mitsubishi Kasei, Japan), was kept as low as possible (usually less than 3 × 10^{−3} mol kg^{−1}). The absorption spectra obtained were analyzed to determine the equilibrium constant of the axial ligand substitution reaction using the SPECFIT/32 program [38]. The unit of mol kg^{−1} is used in the present work instead of mol dm^{−3} because the value of the concentration given on the latter unit depends on the temperature.

3. Results

3.1. UV–Vis absorption spectra of chromium(III) porphyrin complexes

It has been demonstrated that the Cr(III) porphyrin complex having a Cl[−] ligand at the axial coordination site exists as [Cr(porphyrin)(Cl)(L)] in a non-coordinating organic solvent such as dichloromethane and toluene, where L represents a non-charged ligand such as H₂O, pyridine, and 1-methylimidazole [6]. The UV–Vis absorption spectra of [Cr(TPP)(X)(H₂O)] (X = F, Cl, Br) in dichloromethane are shown in Fig. S1. The chemical bond between the Cr and Cl atoms is strong enough to not be broken by adding a strongly coordinating ligand such as 1-methylimidazole. However, under more vigorous conditions, such as chromatographic purification on activated alumina, there exists some evidence for the dissociation of the Cl[−] ligand from [Cr(TPP)(Cl)(H₂O)]. The treatment of the eluted green band from the column of the activated alumina with perchloric acid could transfer the Cr(III)–TPP complex to the perchlorate salt, which is further converted to [Cr(TPP)(Py)₂]⁺ through the reaction with pyridine [39]. Therefore, it is possible for the Cr–X bond (X = halogen atom) to dissociate during the reaction with a strong Lewis base when the Cr–X bond is not very strong, and this phenomenon was observed for the bromine complex, [Cr(TPP)(Br)(H₂O)], as described below.

As in the case of the chlorine complex, [Cr(TPP)(Cl)(H₂O)], the addition of pyridine to the dichloromethane solution of [Cr(TPP)(F)(H₂O)] causes the red shift of the absorption spectrum of the complex as shown in Fig. 1. The reaction product is stable in solution for at least 1 day. A similar phenomenon was observed for the reaction with 1-methylimidazole in the same solvent. These facts are in accord with the mechanism by which the axial H₂O ligand is replaced by pyridine or 1-methylimidazole to produce [Cr(TPP)(F)(L)] (L = Py, 1-Melm). On the other hand, the spectral change occurs via consecutive reactions after the pyridine ligand is added to the dichloromethane solution of [Cr(TPP)(Br)(H₂O)]. As shown in Fig. 2, the absorption spectrum changes rapidly

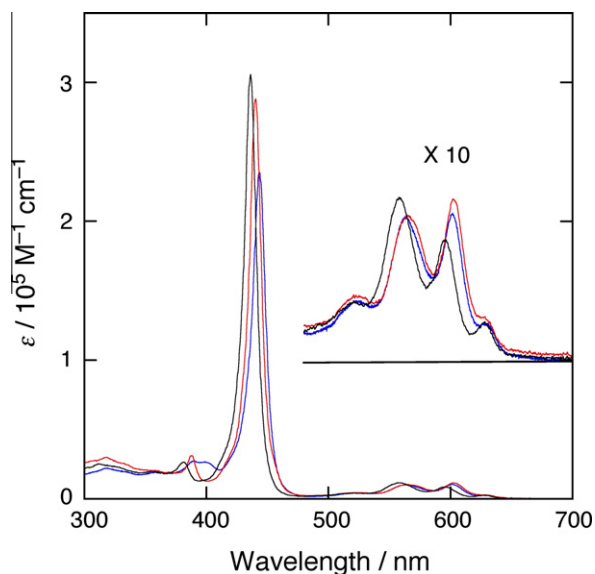


Fig. 1. UV-Vis absorption spectra of the dichloromethane solution of the Cr(III)-TPP complex. [Cr(TPP)(F)(H₂O)] (black), [Cr(TPP)(F)(Py)] (blue), [Cr(TPP)(F)(1-Melm)] (red). (For interpretation of the references to color in this figure legend, the reader is referred to the web version of this article.)

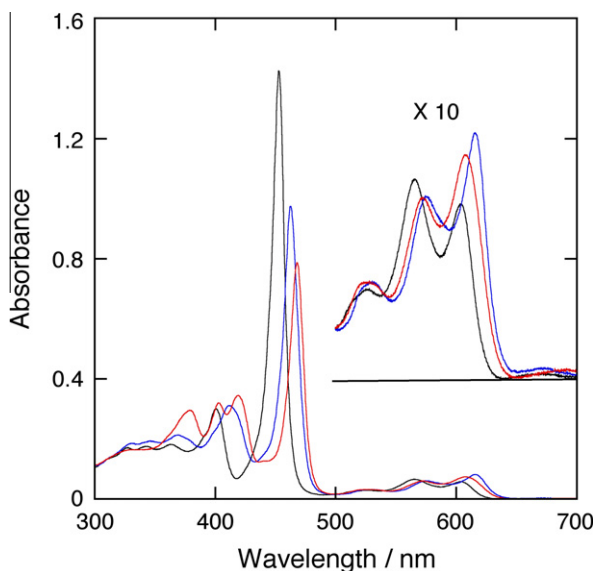


Fig. 2. UV-Vis absorption spectra of the dichloromethane solution of the bromine complex of Cr(III)-TPP. [Cr(TPP)(Br)(H₂O)] (black), the spectrum measured immediately after adding pyridine (blue, [Py] = 4.0×10^{-2} mol kg⁻¹), and the spectrum measured at 120 min after adding pyridine (red). (For interpretation of the references to color in this figure legend, the reader is referred to the web version of this article.)

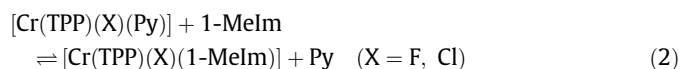
immediately after adding pyridine, followed by a slow spectral shift that occurs over several hours. The initial spectral change resembles that observed for the reaction of pyridine with chlorine and fluorine complexes, while the succeeding spectral change to the final product was observed only for the bromine complex. The spectrum of the final product was identical with that of [Cr(TPP)(Py)₂]⁺, which was prepared independently by the reaction of the perchlorate complex of Cr(III)-TPP with pyridine. It is probable that the bond between the chromium atom and the axial H₂O ligand in [Cr(TPP)(Br)(H₂O)] dissociates more easily in dichloromethane than the bond between the Cr and Br atoms because

the heterolysis of the latter bond should generate an energetically unfavorable charged species in an organic solvent. The mechanism of the two-phase reaction observed here thus can be explained by Chart 1. A similar two-phase reaction was also observed for the reaction of [Cr(TPP)(Br)(H₂O)] with 1-methylimidazole. These findings indicate that the Cr-Br bond is not so strong that coordination of a strong donor ligand at the axial coordination site trans to the bromine atom in [Cr(TPP)(Br)(L)] (L = Py, 1-Melm) may weaken the Cr-Br bond, leading to the dissociation of the bromine atom as Br⁻ ion.

In the case of the chlorine complex, [Cr(TPP)(Cl)(H₂O)], the axial H₂O ligand substitution by the entering ligand such as pyridine is too fast to follow using a stopped-flow spectrophotometer. This is due to the labile nature of the axial H₂O ligand, i.e., the rate constant for the dissociation of H₂O is $k_{-H_2O} = 1.57 \times 10^5$ s⁻¹ at $T = 25.0$ °C [33]. Because a similar situation could be expected for the fluorine complex, [Cr(TPP)(F)(H₂O)], we studied the kinetics of the substitution of the axial pyridine ligand by 1-methylimidazole in [Cr(TPP)(F)(Py)]. The axial ligand substitution reaction of [Cr(TPP)(Br)(L)] is, on the other hand, complicated due to the dissociation of the axial bromine atom, and the kinetics of the ligand substitution reaction was not investigated in the bromine complex.

3.2. Equilibria and kinetics of the axial substitution reaction

It is known that the substitution reaction of the axial ligand of the Cr(III) porphyrin complex by the entering ligand occurs relatively fast in non-coordinating organic solvents [6]. In the present study, we investigated the reaction represented by Eq. (2) in dichloromethane by means of the spectrophotometric method.



We previously studied the substitution reaction of pyridine in [Cr(TPP)(Cl)(Py)] [11–13], and therefore we focused on the substitution reaction of [Cr(TPP)(F)(Py)] in the present study. The equilibrium constant K for reaction 1 (Eq. (2)) was determined by a conventional spectrophotometric method. Spectrophotometric titration of the [Cr(TPP)(F)(Py)] solution with 1-methylimidazole in the presence of a large excess of pyridine over the complex shows that the initial pyridine complex with a Soret band at 443.4 nm was converted into a species with a Soret band at 440.4 nm with isosbestic points as shown in Fig. S2 as an example. Equilibrium constants were determined by simultaneously analyzing the UV-Vis absorption spectra between 300 and 800 nm as a function of the concentrations of leaving and entering ligands using the SPECFIT/32 program [38]. The obtained equilibrium constant for reaction 1 (Eq. (2)) is $(1.97 \pm 0.15) \times 10^2$ at 15.0 °C, $(1.87 \pm 0.11) \times 10^2$ at 25.0 °C, and $(1.57 \pm 0.12) \times 10^2$ at 35.0 °C. The thermodynamic parameters ΔH^0 and ΔS^0 determined by van't Hoff plot of $\ln K$ versus T^{-1} (K⁻¹) were $\Delta H^0 = -8.4 \pm 1.6$ kJ mol⁻¹ and $\Delta S^0 = 15.0 \pm 5.3$ J K⁻¹ mol⁻¹.

Rate constants of the substitution reaction of pyridine on [Cr(TPP)(F)(Py)] by 1-methylimidazole were determined using a stopped-flow spectrophotometer. The progress of the ligand substitution reaction was followed by monitoring the absorbance change after mixing the solution of 1-methylimidazole with that of [Cr(TPP)(F)(Py)], which was prepared by dissolving [Cr(TPP)(F)(H₂O)] into the dichloromethane solution of pyridine. The rate constant was measured under various conditions where 1-methylimidazole and pyridine were present in large excess over the porphyrin complex. The reaction was first order with respect to the porphyrin complex. As shown in Fig. S3, the pseudo-first-order rate constant, k_{obsd} , increased with an increase in the concentration of 1-methylimidazole and then leveled off at higher concentrations

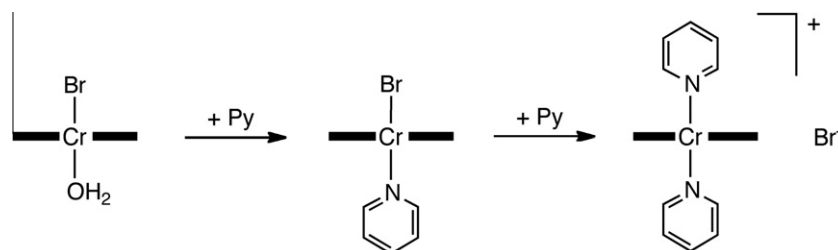


Chart 1. Reaction of $[\text{Cr}(\text{TPP})(\text{Br})(\text{H}_2\text{O})]$ with Py.

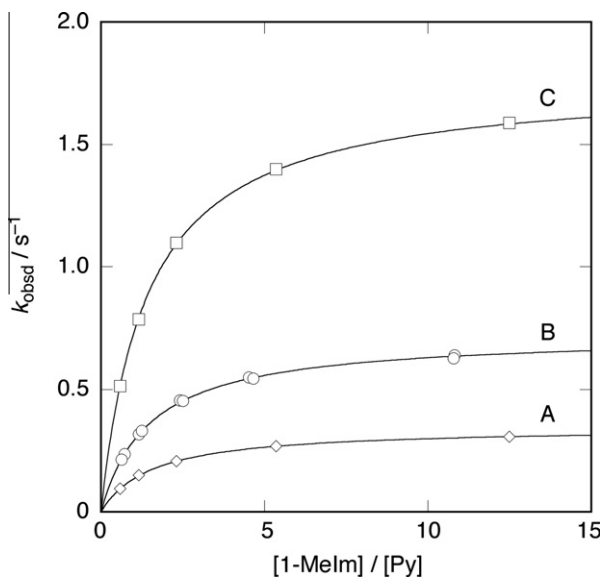
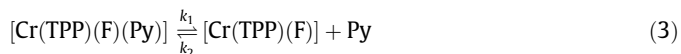


Fig. 3. Dependence of the pseudo-first-order rate constant k_{obsd} on the ratio of $[1\text{-Melm}]/[\text{Py}]$ at $T = 15.0\text{ }^\circ\text{C}$ (A), $25.0\text{ }^\circ\text{C}$ (B), and $35.0\text{ }^\circ\text{C}$ (C). The concentration of the $\text{Cr}(\text{III})$ –TPP complex is $(0.3\text{--}1.0) \times 10^{-5}\text{ mol kg}^{-1}$. Total concentrations of 1-methylimidazole and pyridine are in the range of $1 \times 10^{-3}\text{--}5 \times 10^{-2}\text{ mol kg}^{-1}$. The solid curves were calculated by using the activation parameters obtained.

at a constant concentration of pyridine, while the rate decreased with an increase in the concentration of pyridine at a constant concentration of 1-methylimidazole. The pseudo-first-order rate constant is plotted against the ratio of the concentrations of entering and leaving ligands in Fig. 3. These features of the dependence of the rate constant of the substitution reaction on the ligand concentrations can be interpreted by a dissociative mechanism shown by Eqs. (3) and (4) [13].



When the steady-state approximation is applied to the pentacoordinate intermediate $[\text{Cr}(\text{TPP})(\text{F})]$, the pseudo-first-order rate constant can be expressed as Eq. (5).

$$K_{\text{obsd}} = (k_1 k_3 [1\text{-Melm}] + k_2 k_4 [\text{Py}]) / (k_3 [1\text{-Melm}] + k_2 [\text{Py}])^{-1} \quad (5)$$

Because the k_4 value that corresponds to the intercept of the plot in Fig. 3 is too small to be determined accurately, its value was estimated using the relationship of $K = k_1 k_2^{-1} k_3 k_4^{-1}$. Values of k_1 and $k_2 k_3^{-1}$ at each temperature were determined by fitting the k_{obsd} obtained at various concentrations of pyridine and 1-methylimidazole to Eq. (6) using a least-squares fitting program.

$$K_{\text{obsd}} = k_1 [1\text{-Melm}] / ([1\text{-Melm}] + k_2 k_3^{-1} [\text{Py}])^{-1} \quad (6)$$

Table 1

Kinetic parameters^a for the pyridine substitution reaction of $[\text{Cr}(\text{TPP})(\text{X})(\text{Py})]$ ($\text{X} = \text{F}, \text{Cl}$) by 1-methylimidazole at $T = 25.0\text{ }^\circ\text{C}$.

	$[\text{Cr}(\text{TPP})(\text{F})(\text{Py})]$	$[\text{Cr}(\text{TPP})(\text{Cl})(\text{Py})]^b$
k_1 (s^{-1})	$(7.24 \pm 0.06) \times 10^{-1}$	1.66 ± 0.05
ΔH_1^\ddagger	57.5 ± 1.1	97.2 ± 1.4
ΔS_1^\ddagger	-54.3 ± 3.5	85.1 ± 4.5
k_2/k_3	1.49 ± 0.03	1.68 ± 0.04
$\Delta H_2^\ddagger - \Delta H_3^\ddagger$	-2.9 ± 2.3	2.3 ± 1.2
$\Delta S_2^\ddagger - \Delta S_3^\ddagger$	-6.3 ± 7.6	12.0 ± 3.9
k_4 (s^{-1})	2.6×10^{-3c}	4.13×10^{-3c}
ΔH_4^\ddagger	68.9 ± 3.0	109.8 ± 1.3
ΔS_4^\ddagger	-63.0 ± 9.9	77.7 ± 4.3

^a ΔH (kJ mol^{-1}) and ΔS ($\text{J mol}^{-1}\text{ K}^{-1}$).

^b Reference [13].

^c Calculated by using values of k_1 , k_2/k_3 , and K .

The obtained rate constants are $k_1 = (3.46 \pm 0.05) \times 10^{-1}\text{ s}^{-1}$ at $15.0\text{ }^\circ\text{C}$, $(7.24 \pm 0.06) \times 10^{-1}\text{ s}^{-1}$ at $25.0\text{ }^\circ\text{C}$, $1.76 \pm 0.02\text{ s}^{-1}$ at $35.0\text{ }^\circ\text{C}$, and $k_2 k_3^{-1} = 1.54 \pm 0.05$ at $25.0\text{ }^\circ\text{C}$, 1.49 ± 0.03 at $25.0\text{ }^\circ\text{C}$, $1.42 \pm 0.03\text{ s}^{-1}$ at $35.0\text{ }^\circ\text{C}$. Eyring plots of k_1 and $k_2 k_3^{-1}$ proved linear within experimental error for all reactions. The activation parameters, ΔH^\ddagger and ΔS^\ddagger , were determined by simultaneously fitting the variable-temperature data to Eq. (6) and the Eyring equation. Kinetic parameters thus obtained are summarized in Table 1.

Based on the thermodynamic and kinetic parameters, the effect of the axial halogen ligand on the chemical reactivity of the axial ligand trans to the halogen atom will be discussed in terms of the trans effect. It was revealed that the reactivity of the dissociation reaction of the axial pyridine ligand in $[\text{Cr}(\text{TPP})(\text{X})(\text{Py})]$ ($\text{X} = \text{F}, \text{Cl}$) depends on the nature of the halogen ligand, i.e., the activation enthalpy was determined to be 57.6 kJ mol^{-1} for $\text{X} = \text{F}$ and 97.2 kJ mol^{-1} for $\text{X} = \text{Cl}$. Coordination of the fluorine atom to the chromium atom decreased the activation enthalpy for the pyridine dissociation reaction by ca. 40 kJ mol^{-1} as compared with that of the chlorine complex. A similar effect was observed for the dissociation of 1-methylimidazole. These findings can be ascribed to the stronger bond between the Cr and F atoms than between the Cr and Cl atoms, i.e., the stronger the chemical bond between the metal and coordinating ligand, the weaker the bond trans to it. On the other hand, the activation entropy of the dissociation of pyridine is $-54.4\text{ J mol}^{-1}\text{ K}^{-1}$ for $\text{X} = \text{F}$, which is significantly different from the corresponding value of $85.1\text{ J mol}^{-1}\text{ K}^{-1}$ for $\text{X} = \text{Cl}$. Because the positive value of the activation entropy would be expected for the dissociation of a non-charged ligand such as pyridine from the parent complex, the dissociation of pyridine from the F^- complex should be accompanied with some chemical process that is ascribed to the decrease in activation entropy. Although in the hexacoordinate complex, $[\text{Cr}(\text{TPP})(\text{X})(\text{Py})]$, the polarization of the bond between the chromium and halogen atoms should be compensated by the Cr–N bond trans to the Cr–X bond, the dissociation of pyridine causes the larger polarization of the Cr–X bond in the pentacoordinate intermediate for the F^- complex because the electronegativity of the fluorine atom is much larger than that

of the chromium atom. Such enhanced polarization for the F^- complex during the pyridine dissociation reaction should cause the structure-making effect on the surrounding solvent and/or the association of the water molecules that are included in the dichloromethane solution at the concentration of less than $3 \times 10^{-3} \text{ mol kg}^{-1}$ with the fluorine ligand of the complex through a hydrogen bond, leading to the negative value of the activation entropy. The strength of the bond between the chromium and halogen atoms showed the tendency of $Cr-F > Cr-Cl > Cr-Br$ judging from the findings that the activation enthalpy for the dissociation of the axial pyridine and 1-methylimidazole ligands trans to the F or Cl atom strongly depends on the halogen atom, as well as the two-step reaction observed for the reaction of $[Cr(TPP)(Br)(H_2O)]$ with pyridine, where the cleavage of the bond between the Cr and Br atoms was induced by the introduction of pyridine into the solution. Since the chromium(III) ion is a hard Lewis acid, the tendency of the bond strength between Cr and X (X = F, Cl, and Br) is reasonable.

The trans effect is a kinetic phenomenon and depends on features of both transition and ground states, i.e., the stabilization of the transition state and the weakening of the bond between the metal and the leaving group due to the remaining ligand trans to the leaving group in the ground state, respectively. The trans effect was originally discussed with regard to square planar complexes such as those of Pt(II), where the ligand substitution reactions occur via an associative mechanism [40]. In such a case, the labilization of the leaving ligand may not necessarily be accompanied by the weakening of the bond between the metal ion and the leaving group [41]. On the other hand, in the case of the dissociatively activated ligand substitution reaction, the strengthening of the chemical bond between the metal atom and the ligand trans to the leaving group causes both the weakening of the bond to the leaving group and the stabilization of the transition state of the reaction, and a close relationship between these two factors can be expected for the σ -bonding ligand. One example of such a relationship can be seen in the axial ligand substitution of cobaloximes [42]. The substitution reaction of the axial methanol ligand in cobaloximes occurs via a dissociative mechanism, and the rate of the substitution is enhanced with increasing σ -electron donating ability of the ligand trans to the leaving methanol ligand in the order of $p\text{-CH}_3\text{C}_6\text{H}_4\text{SO}_3^- < (\text{CH}_3)_2\text{PO} < \text{SO}_3^{2-} < \text{C}_6\text{H}_5^- < \text{CH}_3^-$. In such cases the trans effect is usually observed in the rate constant of the substitution reaction. On the other hand, the rate constant of the dissociation reaction of pyridine in $[Cr(TPP)(X)(Py)]$ (X = F, Cl) shows similar values of $k_1 = 1.66 \text{ s}^{-1}$ for X = Cl and $k_1 = 0.724 \text{ s}^{-1}$ for X = F ($T = 25.0 \text{ }^\circ\text{C}$). The coincidence of these k_1 values for both reaction systems may be by chance, and a large difference in the activation enthalpy of the k_1 value for X = Cl and F as mentioned above ($-39.6 \text{ kJ mol}^{-1}$) is compensated by the difference in the activation entropy ($-139.5 \text{ J mol}^{-1} \text{ K}^{-1}$), leading to a small difference in the activation energy of 2.0 kJ mol^{-1} at $T = 25.0 \text{ }^\circ\text{C}$.

Appendix A. Supplementary material

Supplementary data associated with this article can be found, in the online version, at <http://dx.doi.org/10.1016/j.ica.2012.04.001>.

References

- [1] E.B. Fleischer, M. Krishnamurthy, *J. Am. Chem. Soc.* 93 (1971) 3784.
- [2] E.B. Fleischer, M. Krishnamurthy, *J. Coord. Chem.* 2 (1972) 89.
- [3] M. Krishnamurthy, *Inorg. Chim. Acta* 26 (1978) 137.
- [4] K.R. Ashley, J.G. Leopoldt, V.K. Joshi, *Inorg. Chem.* 19 (1980) 1608.
- [5] J.G. Leopoldt, S.S. Basson, D.R. Rabie, *J. Inorg. Nucl. Chem.* 43 (1981) 3239.
- [6] P. O'Brien, D.A. Sweigart, *Inorg. Chem.* 21 (1982) 2094.
- [7] J.G. Leopoldt, R. van Eldik, H. Kelm, *Inorg. Chem.* 22 (1983) 4146.
- [8] J.G. Leopoldt, H. Meyer, *Polyhedron* 6 (1987) 1361.
- [9] K.R. Ashley, J. Kuo, *Inorg. Chem.* 27 (1988) 3556.
- [10] K.R. Ashley, I. Trent, *Inorg. Chim. Acta* 163 (1989) 159.
- [11] M. Inamo, T. Sumi, N. Nakagawa, S. Funahashi, M. Tanaka, *Inorg. Chem.* 28 (1989) 2688.
- [12] M. Inamo, S. Sugiura, H. Fukuyama, S. Funahashi, *Bull. Chem. Soc. Jpn.* 67 (1994) 1848.
- [13] M. Inamo, K. Nakajima, *Bull. Chem. Soc. Jpn.* 71 (1998) 883.
- [14] E.B. Fleischer, S. Jacobs, L. Mesticelli, *J. Am. Chem. Soc.* 90 (1968) 2527.
- [15] R.F. Pasternack, M.A. Cobb, *Biochem. Biophys. Res. Commun.* 51 (1973) 507.
- [16] E.B. Fleischer, M. Krishnamurthy, *Ann. NY Acad. Sci.* 206 (1973) 32.
- [17] R.F. Pasternack, M.A. Cobb, *J. Inorg. Nucl. Chem.* 35 (1973) 4327.
- [18] K.R. Ashley, M. Berggren, M. Cheng, *J. Am. Chem. Soc.* 97 (1975) 1422.
- [19] R.F. Pasternack, M.A. Cobb, N. Sutin, *Inorg. Chem.* 14 (1975) 866.
- [20] K.R. Ashley, S. Au-Young, *Inorg. Nucl. Chem.* 15 (1976) 1937.
- [21] R.F. Pasternack, G.R. Parr, *Inorg. Chem.* 15 (1976) 3087.
- [22] K.R. Ashley, *J. Inorg. Nucl. Chem.* 39 (1976) 357.
- [23] K.R. Ashley, J.G. Leopoldt, *Inorg. Chem.* 20 (1981) 2326.
- [24] J.G. Leopoldt, S.S. Basson, G.J. Lamprecht, R.D. Rabie, *Inorg. Chim. Acta* 51 (1981) 67.
- [25] S. Funahashi, M. Inamo, K. Ishihara, M. Tanaka, *Inorg. Chem.* 21 (1982) 447.
- [26] A. Mahmood, H. Liu, J.G. Jones, J.O. Edwards, D.A. Sweigart, *Inorg. Chem.* 27 (1988) 2149.
- [27] M. Krishnamurthy, *Inorg. Chim. Acta* 25 (1977) 215.
- [28] K.R. Ashley, S. Shyu, J.G. Leopoldt, *Inorg. Chem.* 19 (1980) 1613.
- [29] M. Inamo, M. Hoshino, K. Nakajima, S. Aizawa, S. Funahashi, *Bull. Chem. Soc. Jpn.* 68 (1995) 2293.
- [30] M. Hoshino, N. Tezuka, M. Inamo, *J. Phys. Chem.* 100 (1996) 627.
- [31] M. Hoshino, T. Nagamori, H. Seki, T. Chihara, T. Tase, Y. Wakatsuki, M. Inamo, *J. Phys. Chem. A* 102 (1998) 1297.
- [32] M. Inamo, M. Hoshino, *Photochem. Photobiol.* 70 (1999) 596.
- [33] M. Inamo, H. Nakaba, K. Nakajima, M. Hoshino, *Inorg. Chem.* 39 (2000) 4417.
- [34] M. Inamo, K. Eba, K. Nakano, N. Itoh, M. Hoshino, *Inorg. Chem.* 42 (2003) 6095.
- [35] M. Inamo, N. Matsubara, K. Nakajima, T.S. Iwayama, H. Okimi, M. Hoshino, *Inorg. Chem.* 44 (2005) 6445.
- [36] M. Inamo, C. Okabe, T. Nakabayashi, N. Nishi, M. Hoshino, *Chem. Phys. Lett.* 445 (2007) 167.
- [37] D.A. Summerville, R.D. Jones, B.M. Hoffman, F. Basolo, *J. Am. Chem. Soc.* 99 (1977) 8195.
- [38] Spectrum Software Associates, Marlborough, MA, USA.
- [39] The molecular structure of $[Cr(TPP)(Py)_2]ClO_4$ was determined by X-ray crystallography, unpublished data.
- [40] R.G. Wilkins, *Kinetics and Mechanism of Reactions of Transition Metal Complexes*, second ed., Wiley-VCH, 1991.
- [41] G. Wilkinson, R.D. Gillard, J.A. McCleverty (Eds.), *Comprehensive Coordination Chemistry*, Pergamon Press, Oxford, 1987. vol. 1.
- [42] L. Seibles, E. Deutsch, *Inorg. Chem.* 16 (1977) 2273.